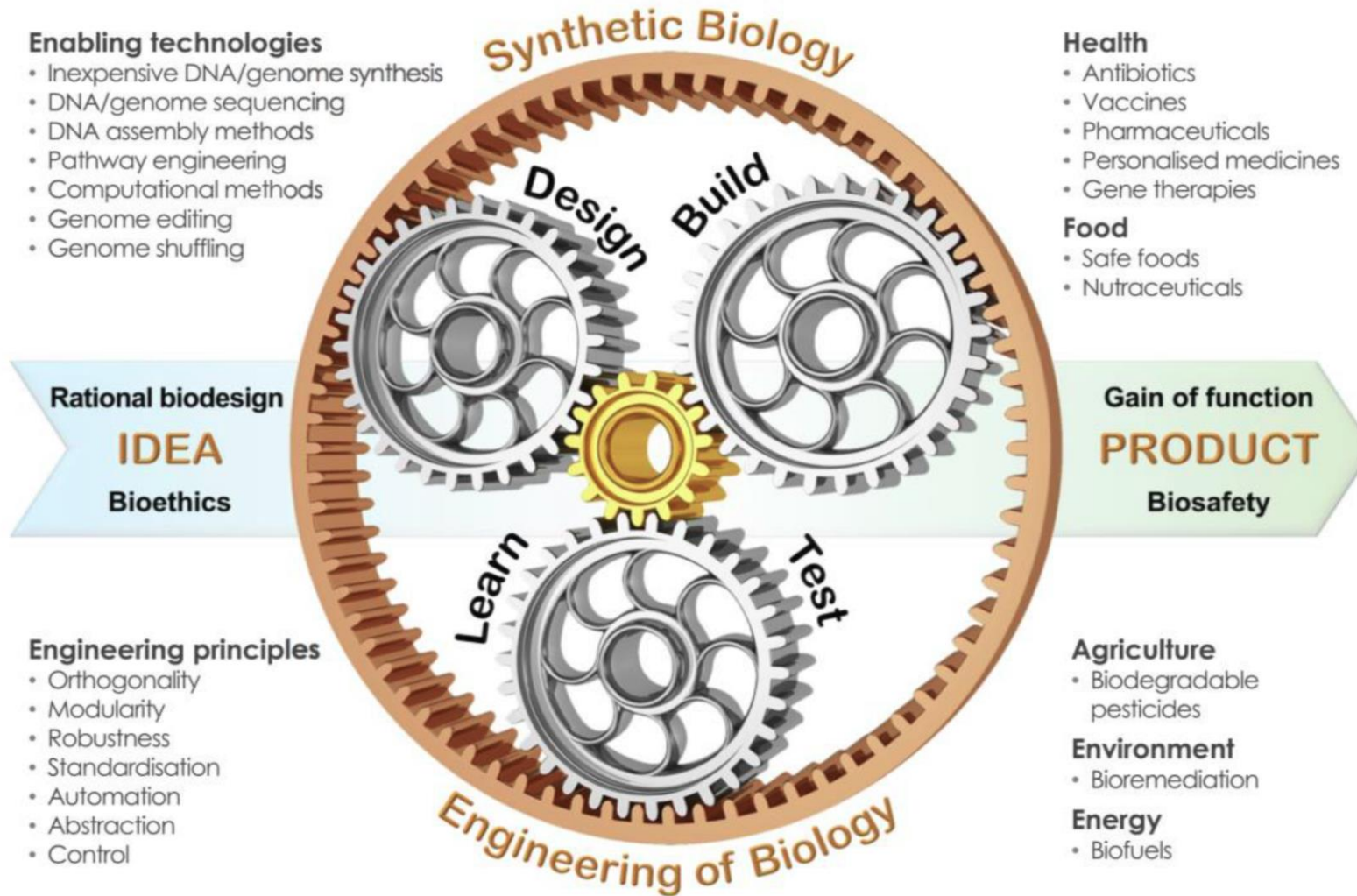


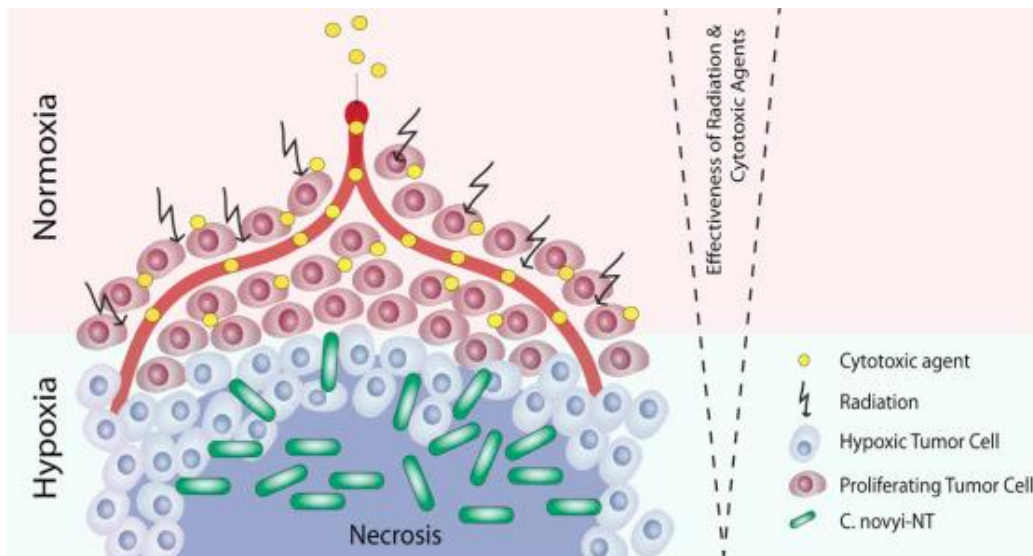
# Applications in synthetic biology



# Tumor targeting bacteria

**Tumor targeting bacteria:** an emerging strategy that represents a viable alternative to molecular targeted therapy and immunotherapy

- Cancer cells within hypoxic areas are dormant but viable and these areas are often responsible for clinical relapse
- Hypoxic areas are poorly accessible to systemically delivered therapeutic and oxygen (important for radiotherapy)
- Hypoxic/necrotic areas are critical niche for bacteria colonization – they are rapidly cleared in the circulation and normal tissues
- Many anaerobic bacteria were shown to target solid tumors – *Salmonella*, *Clostridium*, *Listeria*...



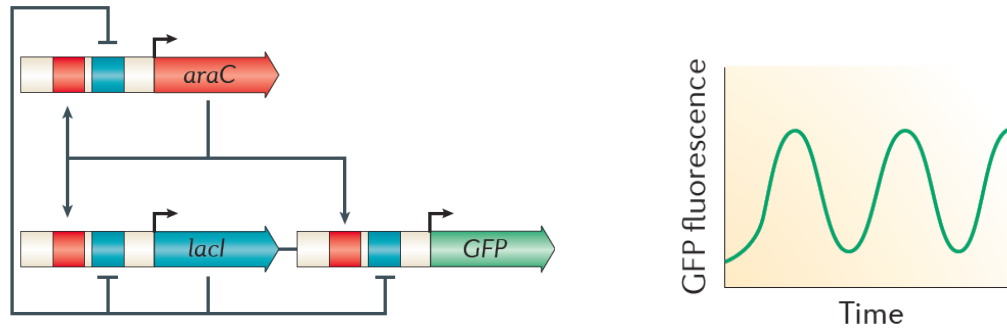
**Engineering towards improving therapeutical potential:**

- **Improving safety** – reducing pathogenicity, exotoxin deletion, ...
- **Increasing tumor targeting** – surface display of antitumor antibodies, systems inducible by tumor-associated factors, ...
- **Effector systems** – cytotoxins, prodrug-converting enzymes, delivery of expression cassettes to targeted cells, expression of tumor antigens or immunomodulators to stimulate immune system (e.g. tetanus toxin)
- **Targeting tumor stroma** – disruption of tumor vasculature, improving bacterial colonization (enzymes degrading extracellular matrix)

*Bacteria programmed to limit bacterial growth while continuously producing and releasing cytotoxic agent*

# Quorum sensing based oscillator

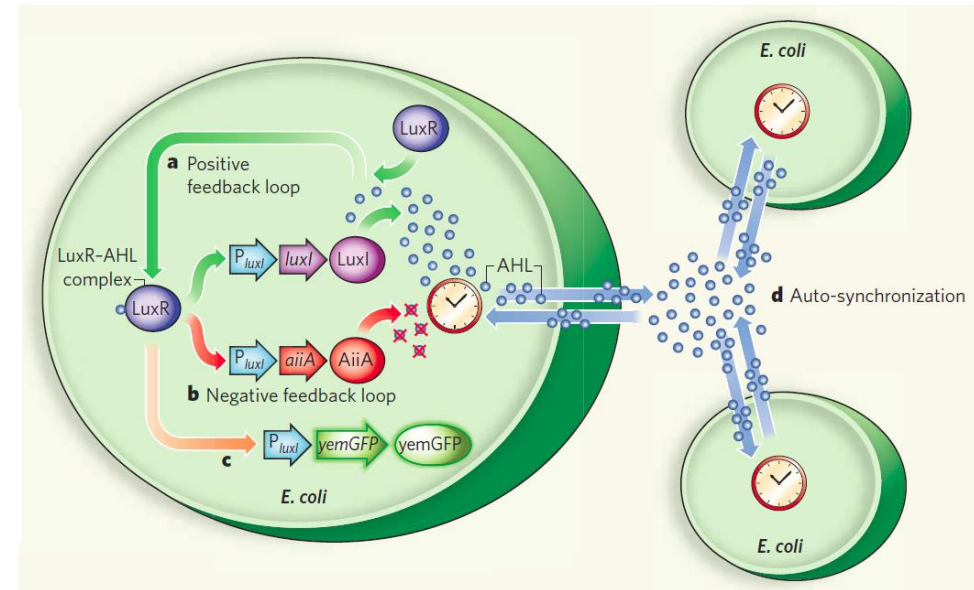
## Positive-negative feedback loop oscillator



- Oscillations are robust, persistent and hereditary
- Oscillations can be adjusted by temperature, growth media, or concentration of transcription inducing molecules
- However, these are still intracellular oscillators – **how to coordinate entire cell populations?**

**Quorum sensing:** communication system between bacteria based on constantly secreted signalling molecules. The concentration of the signal depends on density of the bacteria; when it exceeds a certain threshold, it triggers transcriptional activation that controls some form of collective action (eg biofilm formation).

**Figure 1 | All together now.** Hasty and colleagues<sup>1</sup> have constructed a network of genes and proteins in *Escherichia coli* that acts as a molecular clock and can be synchronized across a population of the bacteria. **a**, When bound to the diffusible molecule acyl-homoserine lactone (AHL), the constitutively expressed LuxR receptor initiates a positive feedback loop by triggering expression of LuxI, the enzyme that synthesizes AHL. The expression of LuxI is driven by  $P_{luxI}$ , a DNA promoter sequence. Large arrows indicate DNA promoter sequences or genes. **b**, The LuxR–AHL complex also kicks off a time-delayed negative feedback loop by activating the  $P_{luxI}$ -driven production of AiiA, a protein that degrades AHL. **c**, In the final section of the network, the LuxR–AHL complex triggers  $P_{luxI}$ -driven expression of a green fluorescent protein (yemGFP). **d**, The dynamic interactions of the positive and negative feedback loops produce regular pulses of AHL, which act as time-keepers in the molecular clock. The AHL molecules diffuse out of each cell and across the membranes of neighbouring bacteria, where they stimulate the expression of yemGFP. All the cells of the *E. coli* population simultaneously send and receive AHL, providing a signal that enables each individual clock to self-adjust and auto-synchronize with the others, as demonstrated by the coordinated pulses of fluorescence produced by the bacteria.





# Bacteria synchronized for drug delivery

*Bacteria programmed to limit bacterial growth while continuously producing and releasing cytotoxic agent*

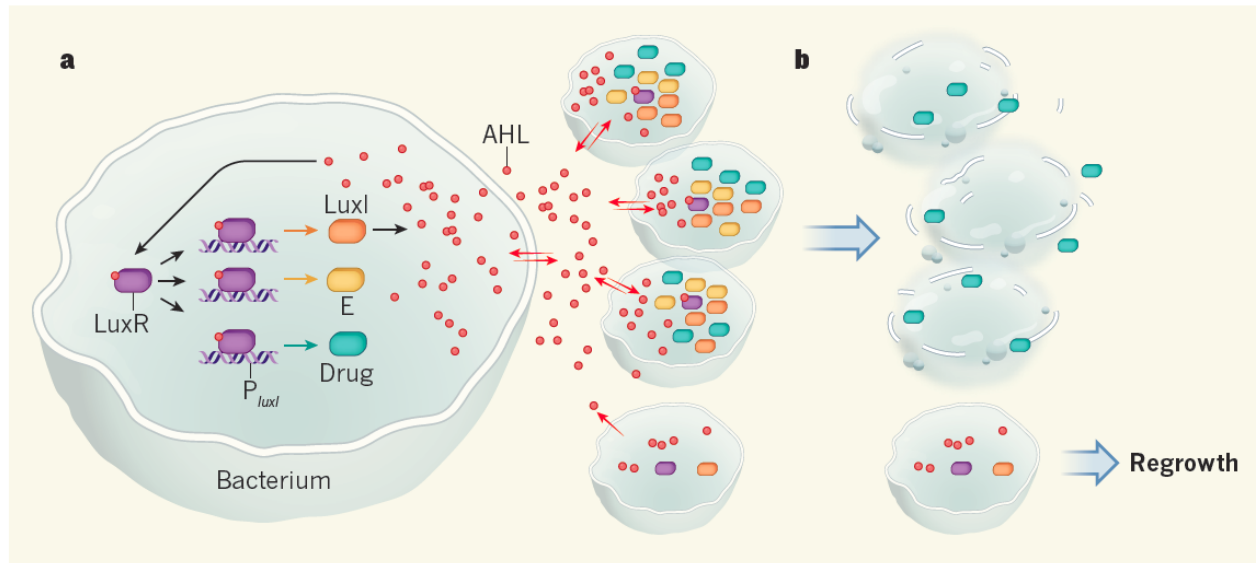


**Figure 1 | Synchronized cyclical lysis and drug release.** Din *et al.*<sup>1</sup> constructed a genetic circuit in tumour-targeting bacteria that mediates drug production and release through cell lysis in synchronized, repeated cycles. **a**, Binding of the signalling molecule AHL to its receptor protein LuxR leads to their subsequent interaction with, and activation of, the promoter DNA sequence  $P_{luxI}$ . This promoter drives expression of the gene that encodes the enzyme LuxI, which catalyses AHL synthesis, thus generating a feed-forward loop. The promoter also drives expression of genes that encode a bacterial toxin (drug) to kill cancer cells, and protein E, which releases the drug through bacterial-cell lysis. AHL can diffuse freely in and out of cells (red arrows). When the density of the bacterial population is low, AHL primarily diffuses out of the cell and the circuit is not active. When population density increases, intracellular AHL accumulates, reaching a threshold concentration that activates the circuit in most cells. **b**, The cells lyse in synchrony, releasing a burst of the drug. The few bacteria that survive kick off another cycle.

## Components:

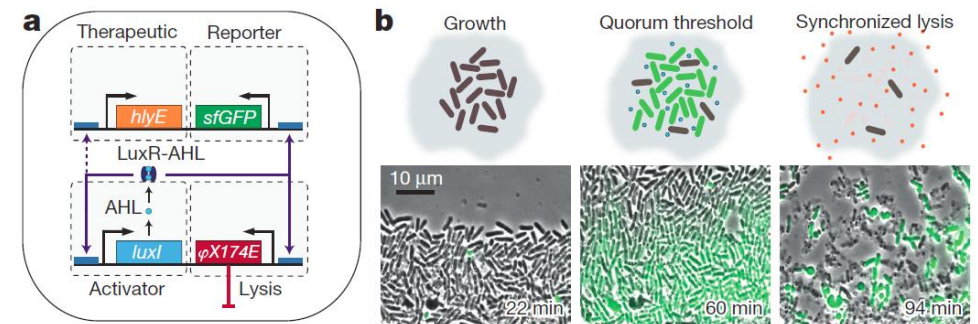
**LuxI** – production of acetyl homoserine lactone (AHL)

**LuxR** – AHL receptor, transcriptional activator

**$\Phi 184 E$**  – bacteria lysis protein

**sfGFP** – superfolder GFP (rapidly folding GFP variant)

**hlyE** – pore forming anti-tumor toxin Haemolysin E



# Remote detection of buried landmines using a bacterial sensor

## Detection of 2,4-dinitrotoluene and 2,4,6-trinitrotoluene residues

Screening of *E.coli* promoter library for response to DNT and TNT



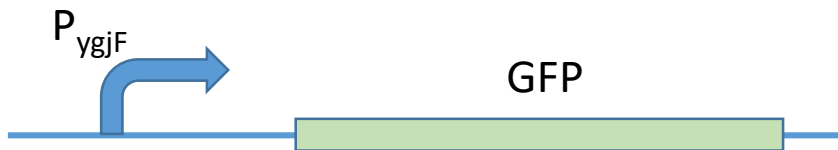
*yqjF* and *ybiJ* promoters  
(detect a volatile products of DNT degradation)



Directed evolution of the *yqjF* promoter



Improved robustness and sensitivity of the *yqjF* promoter



**DNT/TNT bacterial sensor**

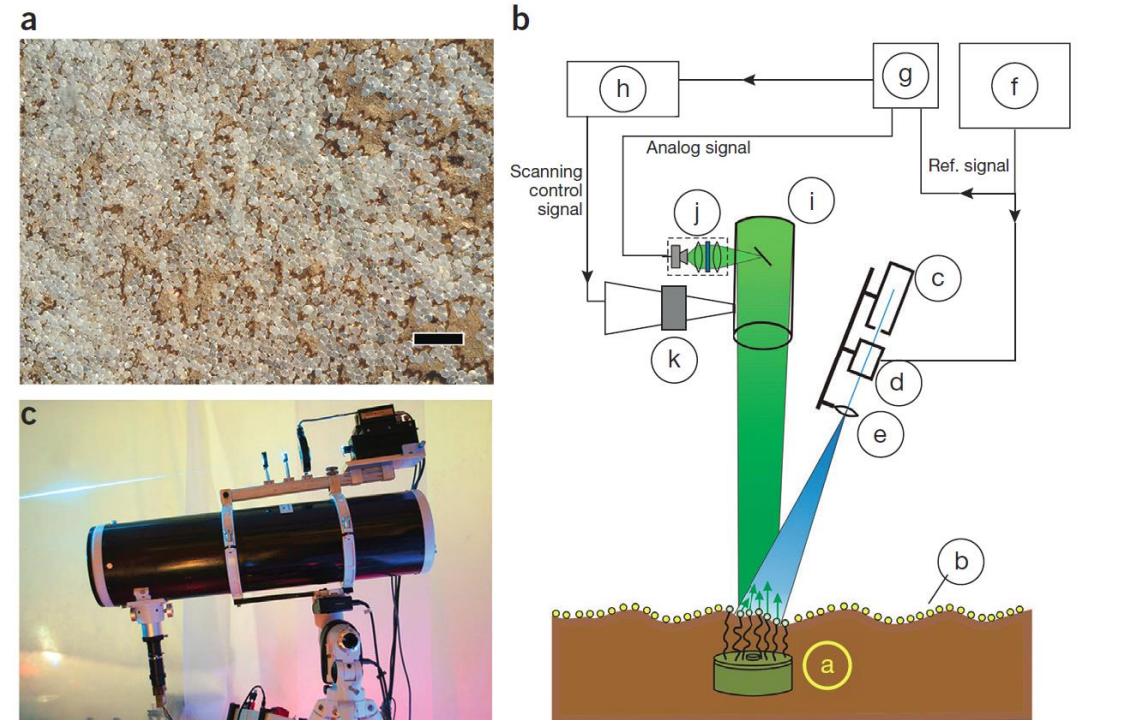


**Figure 1** Optical scanning system and alginate-encapsulated bacterial sensors. (a) Biosensor beads spread over target areas. Scale bar, 2 cm. (b) Schematic of the optical scanning system. Key. (a) Buried landmine; (b) beads containing encapsulated bacteria; (c) laser system producing a Gaussian beam with 0.5 W at 473 nm; (d) laser modulator; (e) optical aiming system; (f) oscillator; (g) digital data acquisition card; (h) computer; (i) collecting telescope; (j) detection module; (k) scanning apparatus. (c) Photograph of the optical scanning system.

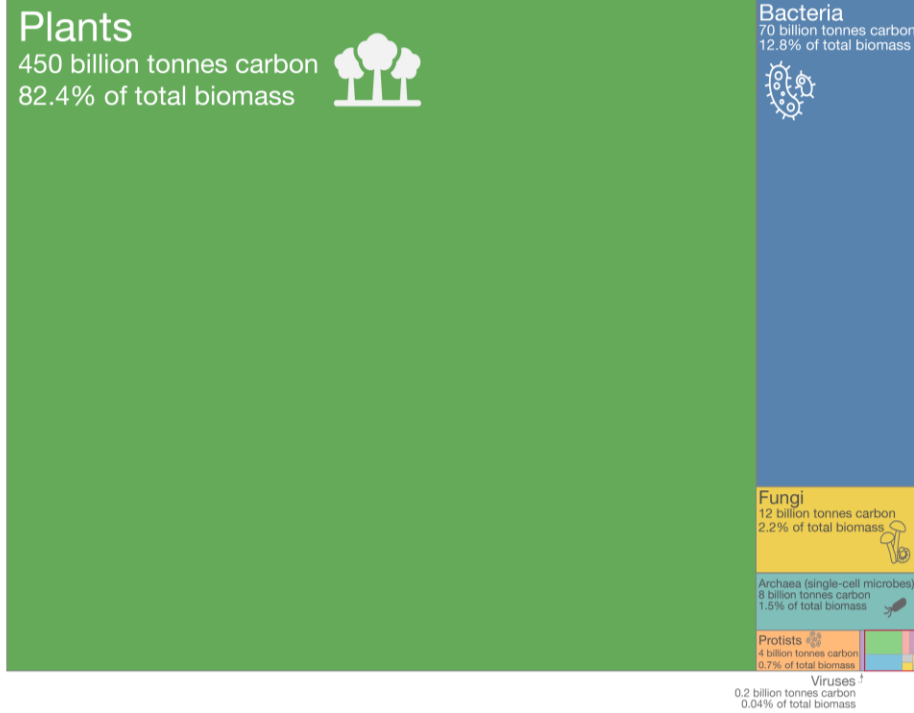
# Applications of synthetic biology in plants



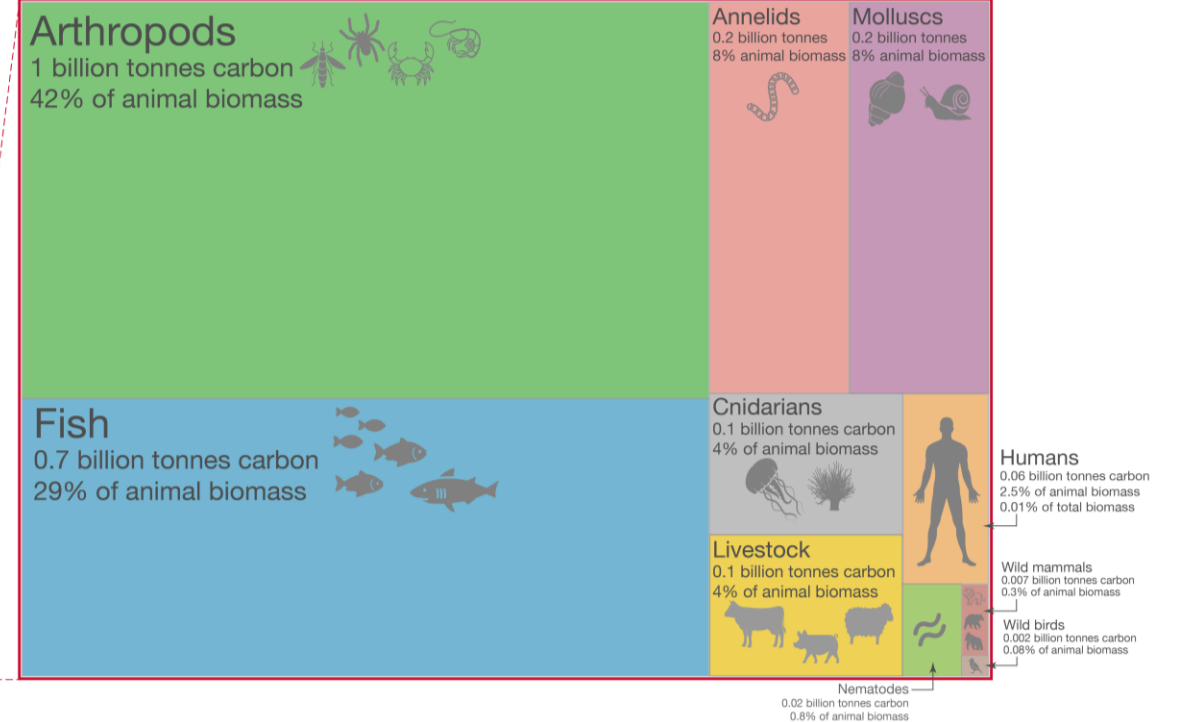


# The distribution of Earth's biomass

Global biomass: 546 billion tonnes of carbon



Animal biomass: 2 billion tonnes of carbon (0.4% of total biomass)

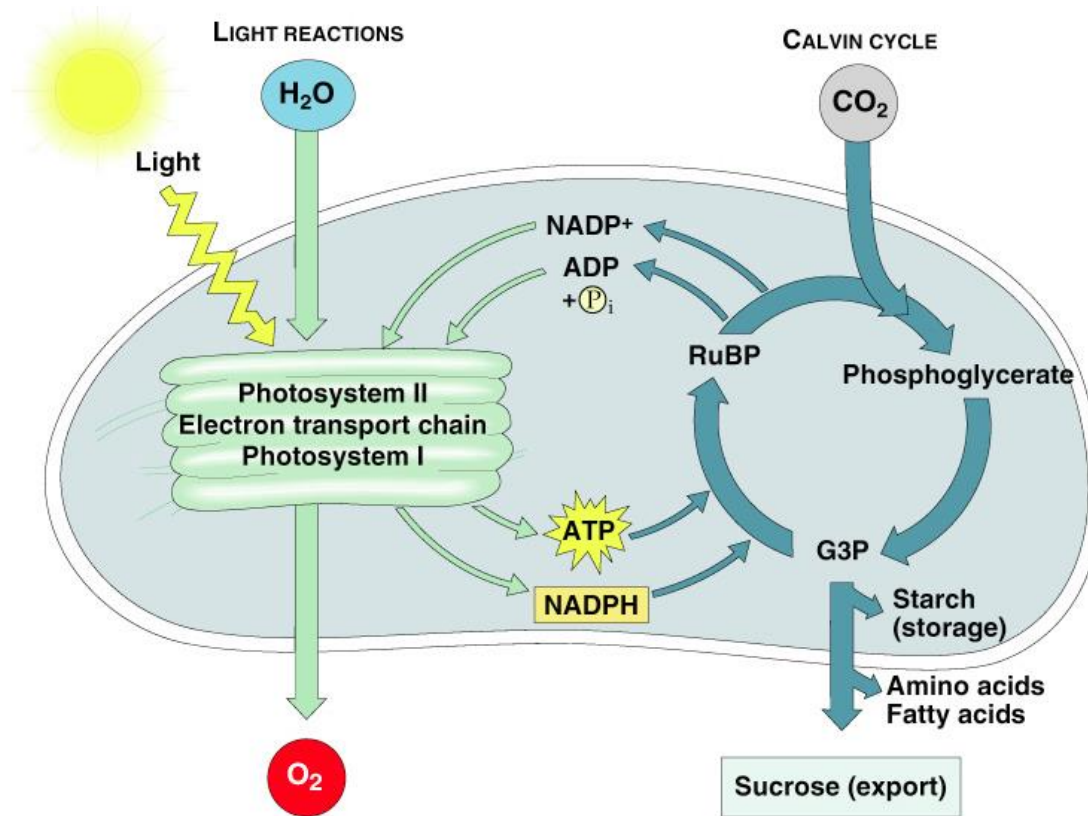
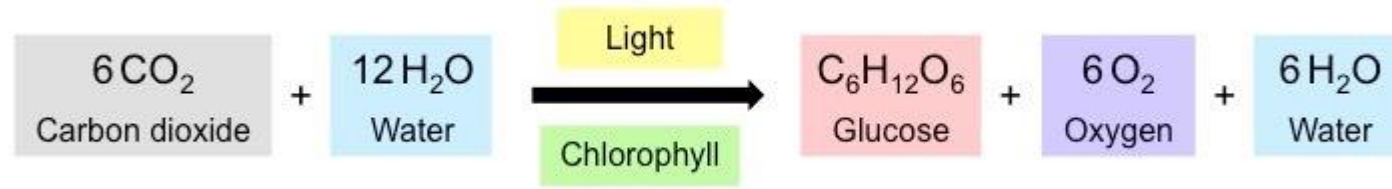


Source: Based on data from Bar-On, Y. M., Phillips, R., & Milo, R. (2018). The biomass distribution on Earth. *Proceedings of the National Academy of Sciences*. Icon graphics sourced from Noun Project (2018). This is a visualization from [OurWorldinData.org](https://ourworldindata.org), where you find data and research on how the world is changing.

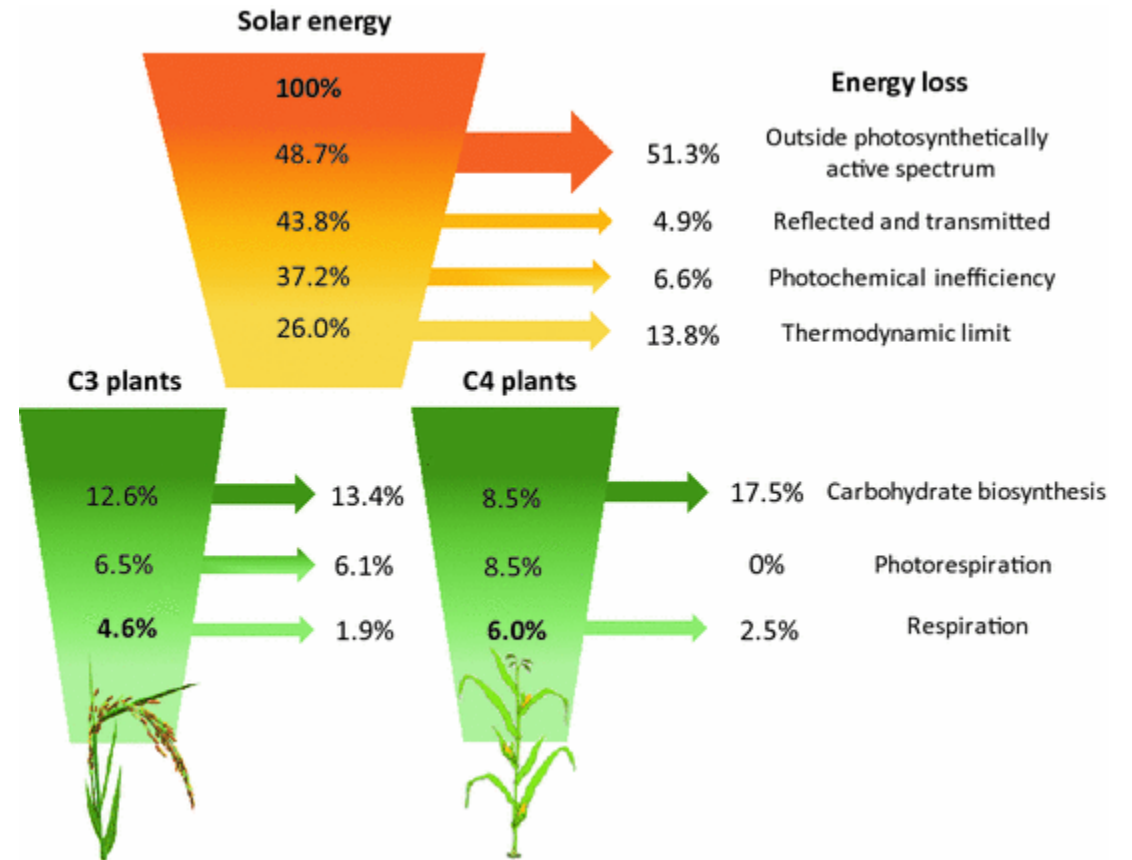
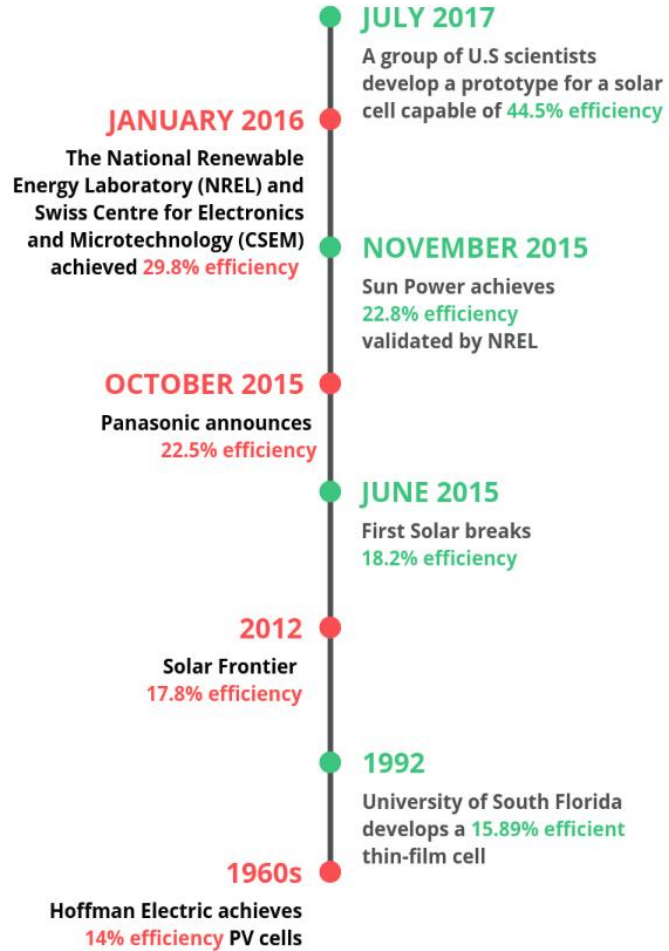
Licensed under CC-BY by the authors Hannah Ritchie and Max Roser (2019).



# Photosynthesis



# Efficiency of photosynthesis



# Do we need to increase efficiency of photosynthesis

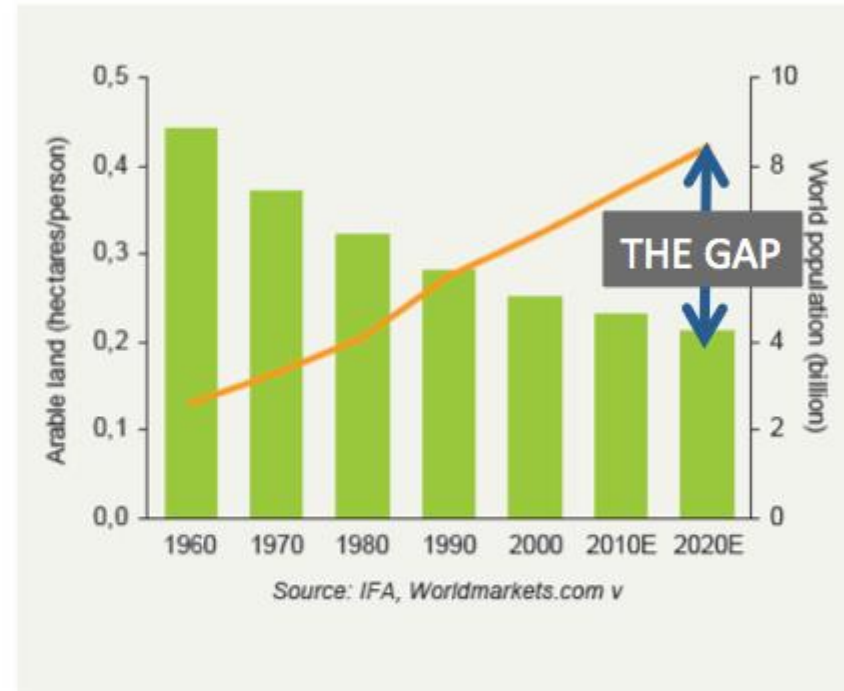
## CLOSE THE GAP!

Very limited potential to increase arable land

Improved living standards increase protein consumption per person requiring more grain for animal feed

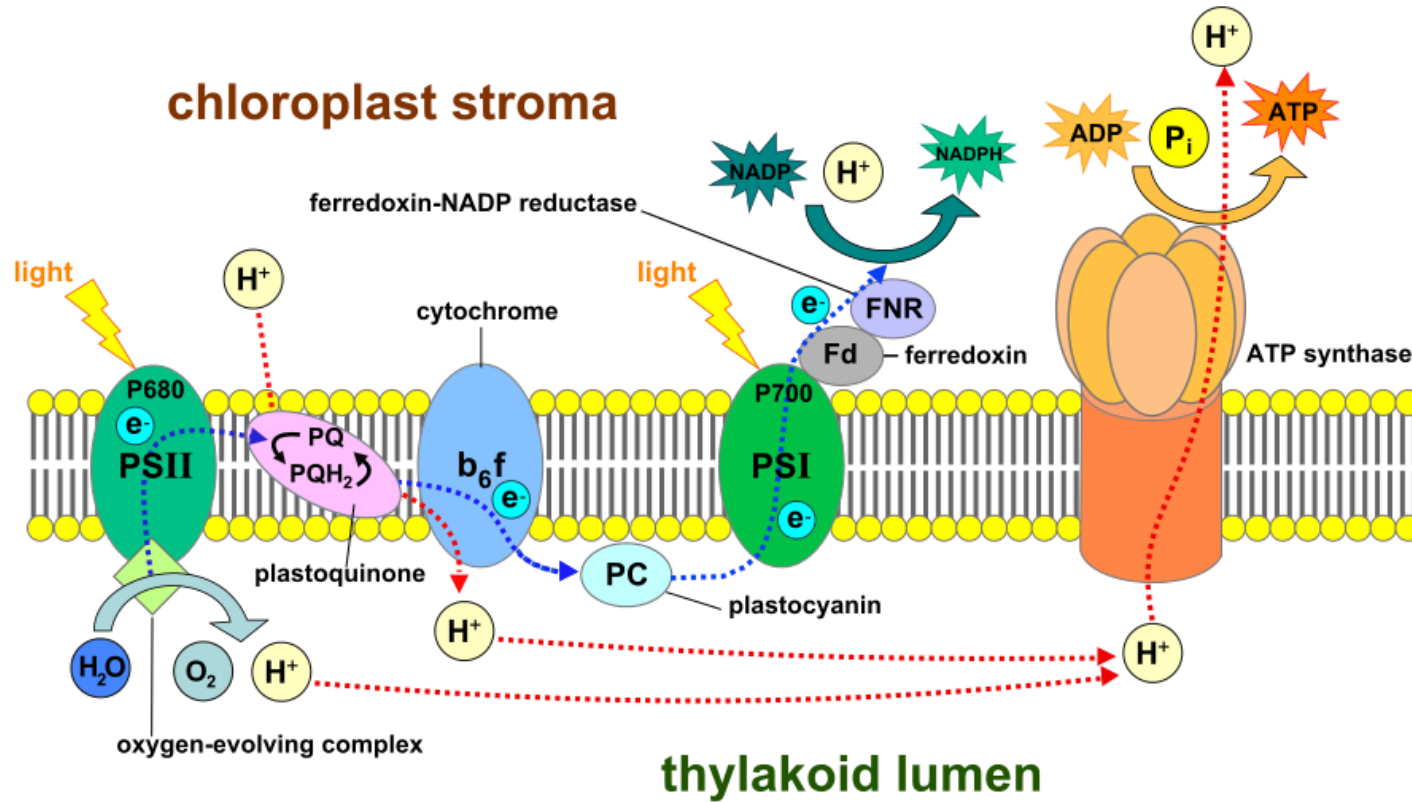


**The only solution is to increase agricultural productivity**



Source: Norman Borlaug statement on the basis of 2005 food production level.

# Photosynthesis: light reaction



Photosystem I (PSI) is naturally adapted for highly efficient light harvesting and charge separation. PSI operates with a quantum yield close to 1, and currently, no synthetic system has approached such remarkable efficiency.



# Light reaction of photosynthesis as target for synthetic biology

1. Enhancement of the process *in vivo* to increase the efficiency of light use to increase biomass and crop yields.

Increasing spectral range at which photosynthesis operates: e.g. cyanobacteria that employ plant-derived LHCs as antennae to shift the light saturation of photosynthesis to higher intensities, or the integration of cyanobacterial chlorophyll d and chlorophyll f (which can absorb far-red and near infrared light) into algal or plant photosynthesis to expand the spectral region available to drive photosynthesis.

2. Coupling of the light reactions of photosynthesis to previously unconnected pathways will enable to utilize the reducing power directly to produce large amounts of high-value compounds *in vivo*.
3. The high efficiency and robustness of PSI should allow it to be used in hybrids with biotic or abiotic components to generate hydrogen, simple carbon-based solar fuels, or electricity *in vitro*.



# Direct coupling to previously unconnected pathways

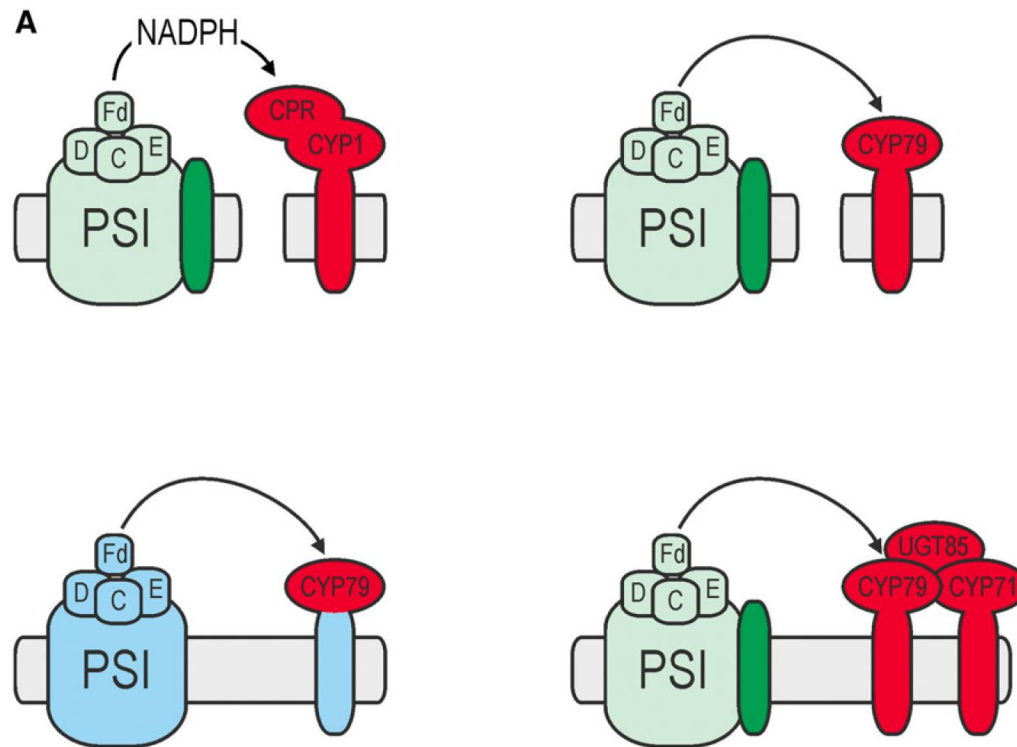
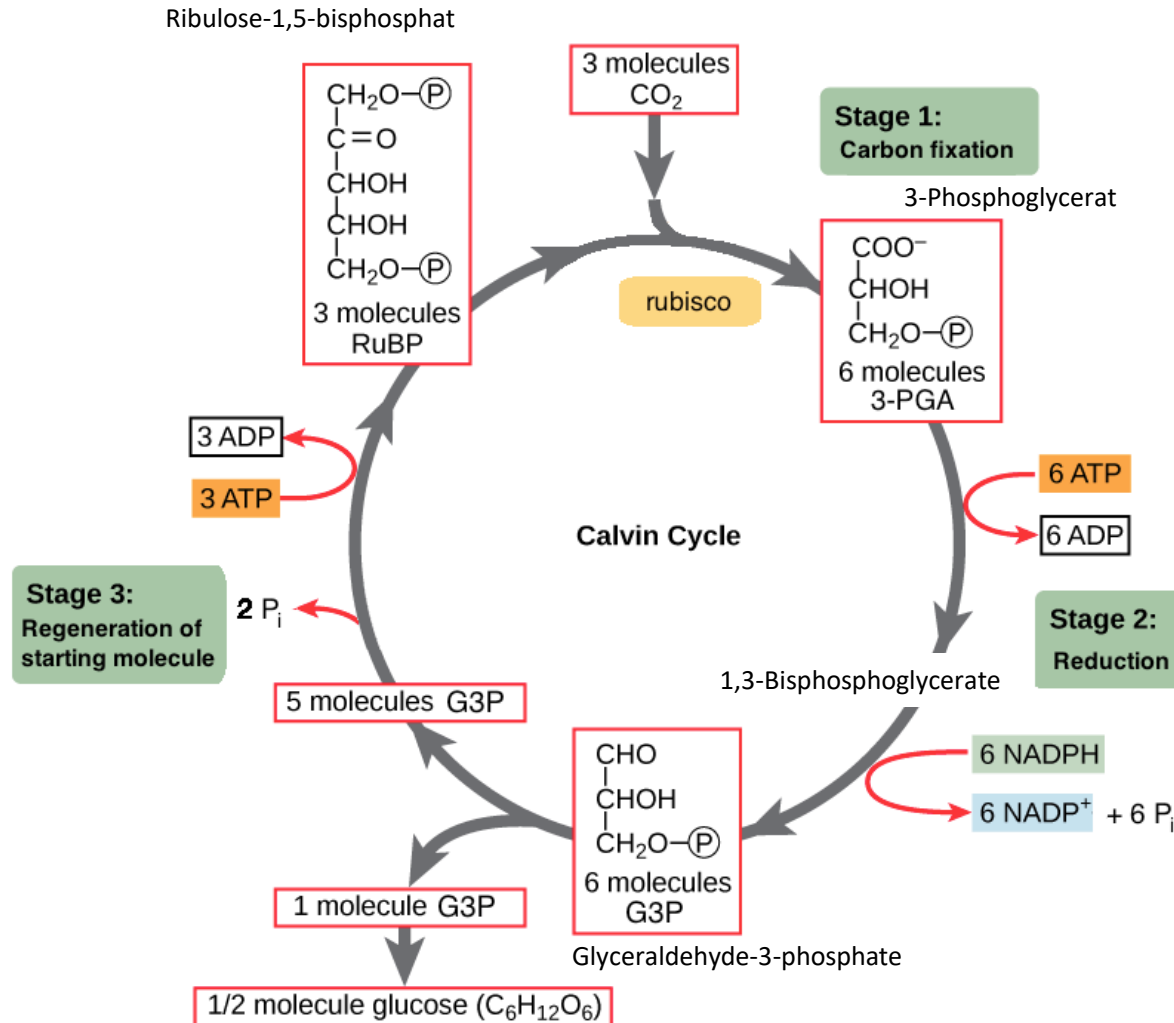


**Figure 4.** Design of bio-bio hybrids. A, Harnessing the reducing power of photosynthesis for cytochrome P450 enzymes (red) has been demonstrated in vitro and in vivo. In vitro approaches were based either on a CPR-CYP1A1 fusion protein that could use NADPH produced by photosynthesis or on CYP79A1 that can utilize photoreduced ferredoxin directly. The latter approach also was realized in vivo by fusing CYP79A1 to ferredoxin (not shown) or the PSI subunit PsaM. The most elaborate approach reported utilizes three enzymes (CYP79A1, CYP71E1, and UGT85B1) to couple dhurrin synthesis with photosynthesis. B, PSI-hydrogenase complexes are based either on genetic fusions of the hydrogenase (Hyd) to PsaE or ferredoxin or on covalent linking of the hydrogenase and PSI via a molecular wire. Currently, these bio-bio hybrids function only in vitro.

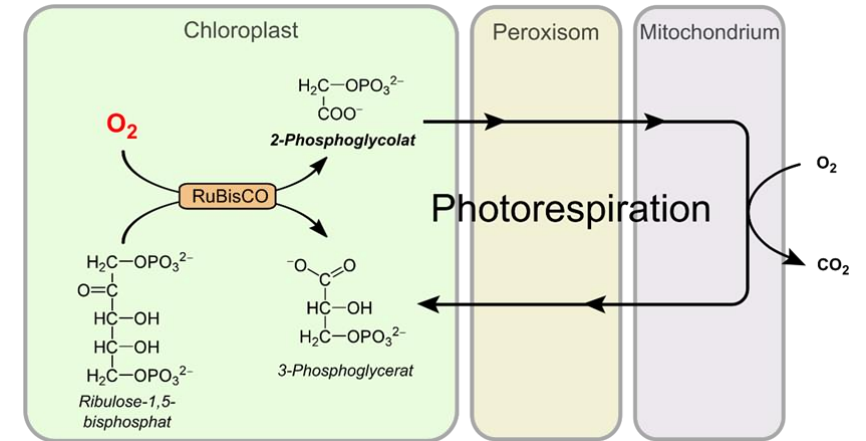
P450s are monooxygenases that insert an oxygen atom into hydrophobic molecules, which enhances their reactivity and hydrophilicity. They act on various endogenous and xenobiotic molecules and their extreme versatility and irreversibility of catalyzed reactions make these enzymes very attractive for use in biotechnology, medicine, and phytoremediation.

Attempts to couple PSI directly with hydrogenases to produce  $H_2$  – fuel cells.

# Photosynthesis: dark reaction



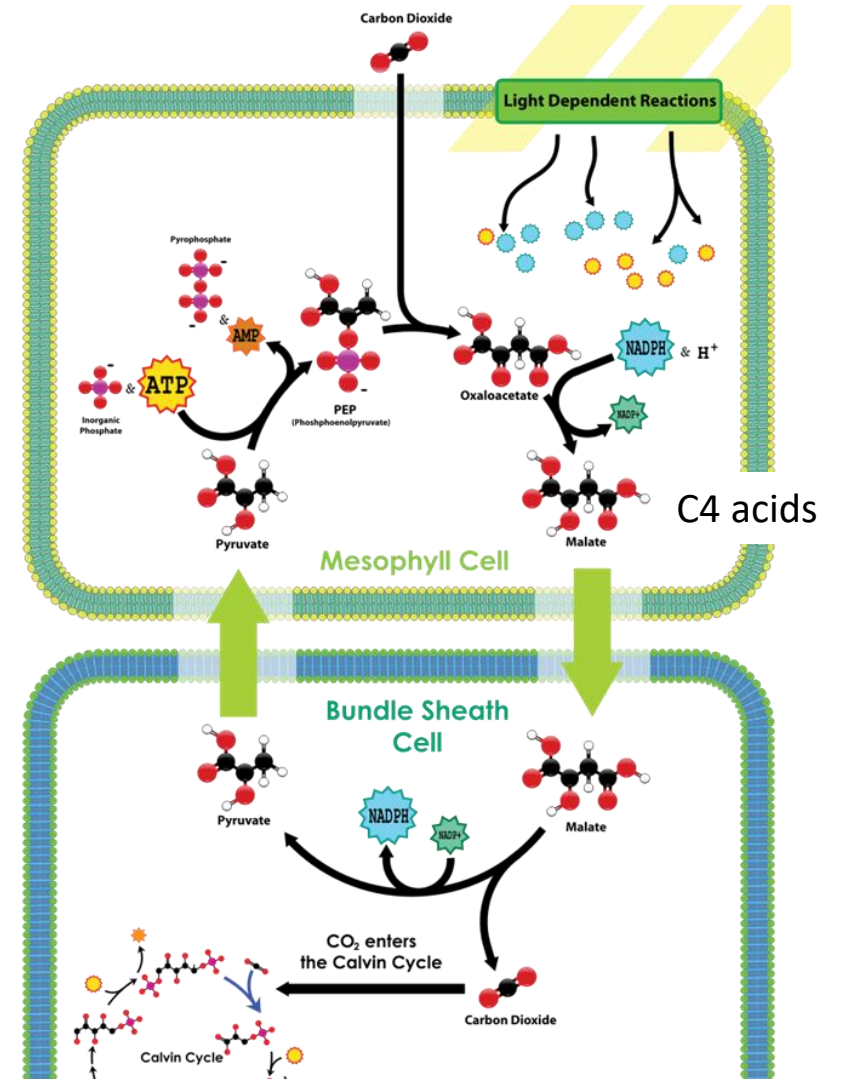
## Oxygenation: up to 25% RuBisCo reactions



Around 25% of carbon fixed by photorespiration is re-released as CO<sub>2</sub> and nitrogen.

# Strategies to improve the dark reaction

- **Engineering RuBisCo** for higher CO<sub>2</sub> specificity (ambient CO<sub>2</sub> concentrations are changing at a rate faster than plants can adapt to them, so replacing plant Rubisco with another variant could boost carbon fixation by up to 25%)
- **Optimizing expression of Calvin cycle enzymes:** at higher CO<sub>2</sub> is regeneration of RuBP rate limiting – Calvin cycle is not optimal and may limit photosynthesis. Specificity. Overexpression of sedoheptulose- 1,7-bisphosphatase and fructose-1,6-bisphosphatase increased photosynthetic rates and biomass in tobacco.
- **Establishing carbon concentrating mechanisms** at the sites of RuBisCo activity to inhibit oxygenation (carboxysomes, pyrenoids)
- **Carbon conserving photorespiration** engineering photorespiration bypass that does not lead to the release of CO<sub>2</sub>
- **Engineering C4 photosynthesis** – independently evolved at least 66 times. It is a complex task that includes alteration of plant tissue anatomy, establishment of bundle sheath morphology, metabolic shuttling of intermediates between cells, as well as ensuring a cell type-specific enzyme expression. Alternative approach is **temporal decoupling** of light and dark reactions whereby malate synthesized during night is stored in vacuoles.

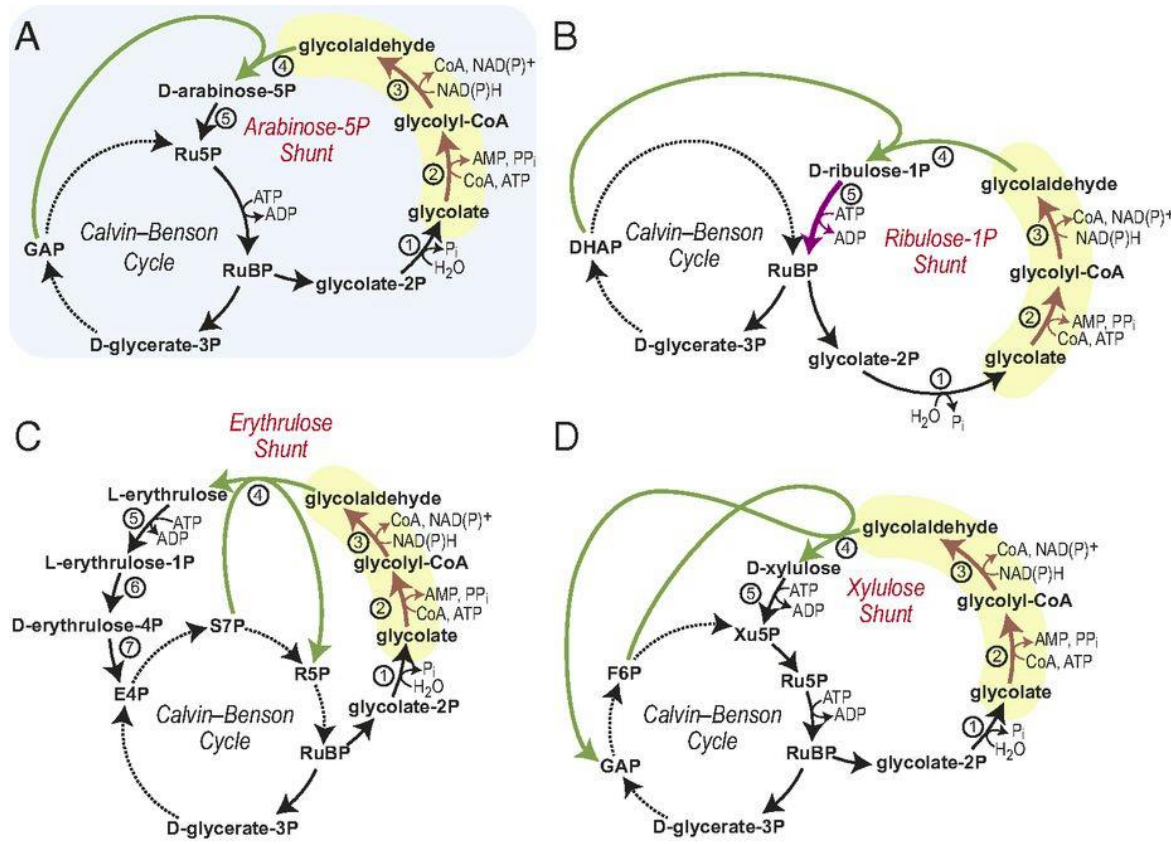


C4 photosynthesis is present in 3% of plants. It utilizes phosphoenolpyruvate carboxylase, the most efficient carbon fixation enzyme.





# Design and *in vitro* realization of carbon-conserving photorespiration

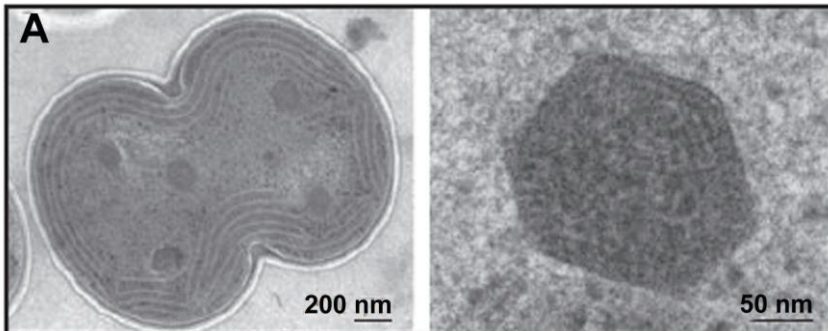
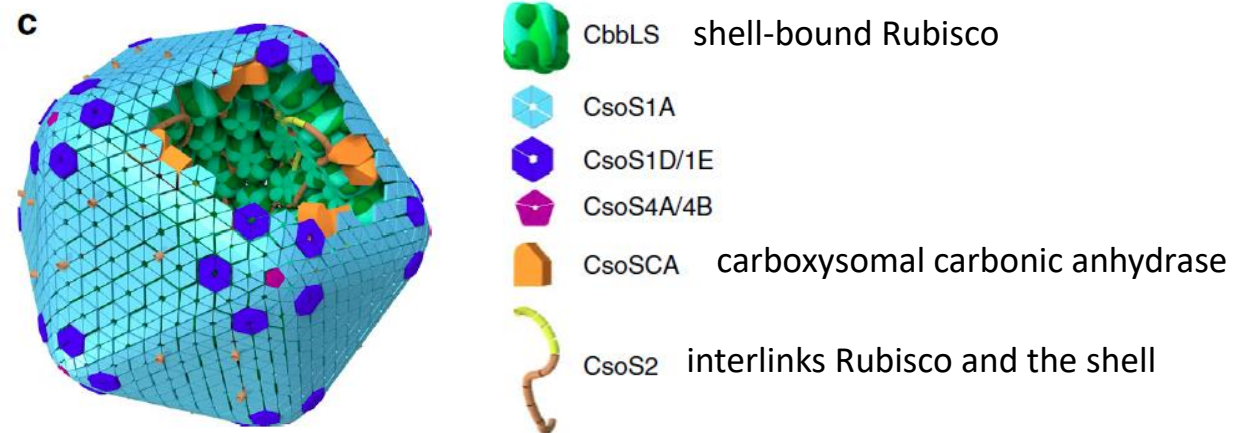
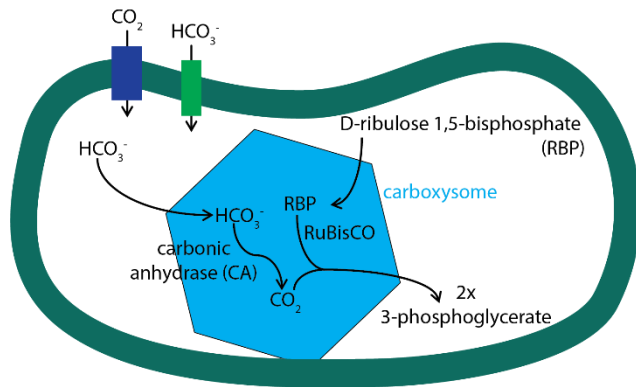


- Metabolic modelling to design possible photorespiration shortcuts that do not release CO<sub>2</sub> (short, energetically feasible, limited overlap to endogenous metabolism)
- Pathway involving reduction of glycolate to glycoaldehyde most promising
- Required engineering novel enzymatic reaction: glycolate reduction to glycoaldehyde
- acetyl-CoA synthetase was engineered toward higher stability and increased catalytic efficiency with glycolate
- NADH-dependent propionyl-CoA reductase was engineered to use NADPH and for >10-fold increased selectivity for glycolyl-CoA over acetyl-CoA
- The glycolate reduction module was validated *in vitro*
- Theoretically, the synthetic pathways described here are expected to support a 10–60% increase in carbon fixation rate, which could provide a dramatic boost in plant growth and productivity.

	①	②	③	④	⑤	⑥	⑦
(A)				fructose-6P aldolase	arabinose-5P isomerase		
(B)			glycolaldehyde dehydrogenase (CoA-acylating)	fucose-1P aldolase	ribulose-1P kinase		
(C)	2-phosphoglycolate phosphatase	glycolyl-CoA synthetase		transketolase	L-eythrulose kinase	L-eythrulose-1P epimerase	D-eythrulose-4P isomerase
(D)				transaldolase	xylulose kinase		
(E)			glycolyl-CoA carboxylase	tartronyl-CoA reductase	tartronate SA reductase	glycerate 3-kinase	

# Carboxysomes in cyanobacteria

The cyanobacterial carbon concentrating mechanism is a single-cell, bipartite system that first generates a high intracellular bicarbonate ( $\text{HCO}_3^-$ ) pool through action of membrane-bound inorganic carbon (Ci) transporters and  $\text{CO}_2$ -converting complexes. This  $\text{HCO}_3^-$  pool is then utilized by subcellular micro-compartments called **carboxysomes**, which encapsulate the cell's complement of Rubisco. The carboxysome's outer protein shell enables diffusional influx of  $\text{HCO}_3^-$  and RuBP, where the former is converted to  $\text{CO}_2$  by a localized carbonic anhydrase (CA).



Carboxysome of *Cyanobium*

# Engineering carboxysomes in tobacco chloroplasts

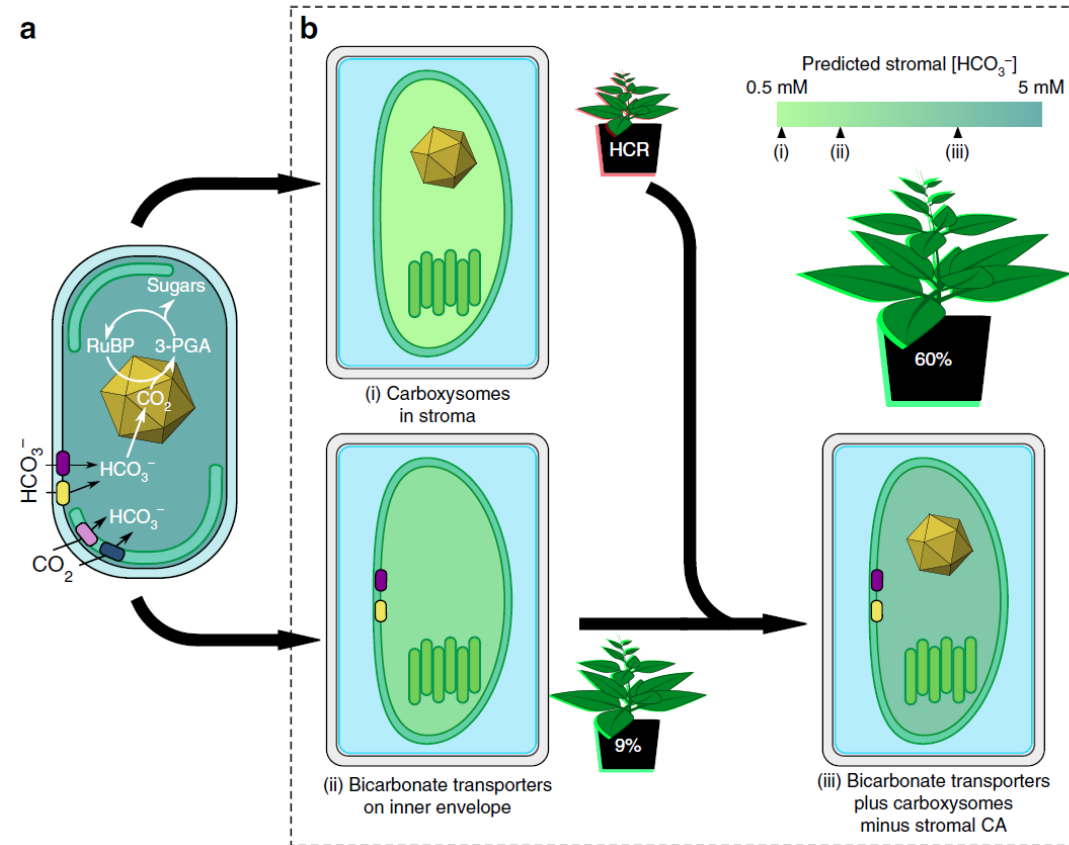


**Fig. 1** Cyanobacterial CCM components for improved photosynthesis. Cyanobacterial CCMs (a) use bicarbonate ( $\text{HCO}_3^-$ ) and  $\text{CO}_2$  pumps on the plasma and thylakoid membranes, respectively, to elevate cytosolic  $\text{HCO}_3^-$ . This  $\text{HCO}_3^-$  pool is utilized by icosahedral-shaped Rubisco microcompartments called carboxysomes (yellow icosahedron), where  $\text{HCO}_3^-$  is converted to  $\text{CO}_2$  by localized carbonic anhydrase (CA) and accumulates due to resistive  $\text{CO}_2$  efflux. The carboxysome encapsulates the cell's complement of a high-catalytic-rate Rubisco, which operates at close to  $V_{\text{max}}$ , converting ribulose-1,5-bisphosphate (RuBP) to 3-phosphoglycerate (3-PGA) within the Calvin cycle. This mechanism leads to efficient photosynthesis and reduced nitrogen allocation compared to  $\text{C}_3$  plants. A strategy to improve  $\text{C}_3$  photosynthesis in plant cells (b, represented here as rectangular structures containing dual-membrane chloroplasts) using the cyanobacterial CCM recommends independent transfer of carboxysomes containing their cognate Rubisco to the chloroplast stroma (i) and  $\text{HCO}_3^-$  pumps (ii) to the chloroplast inner-envelope membrane. Successful transfer of  $\text{HCO}_3^-$  transporters alone (ii) should generate a moderately elevated stromal  $\text{HCO}_3^-$  pool (indicated by the change in colour shading of the chloroplast) and has a predicted photosynthetic improvement of 9%<sup>15</sup> due to the resulting net elevation of  $\text{CO}_2$  near Rubisco. Expression of functional carboxysomes (i), or just their cognate Rubisco, in the chloroplast stroma should lead to a high  $\text{CO}_2$ -requiring (HCR) phenotype due to the characteristically high  $K_M$  and low specificity for  $\text{CO}_2$  of carboxysomal Rubiscos and absence of an elevated  $\text{HCO}_3^-$  or  $\text{CO}_2$  pool. However, in combination (iii), generation of high stromal  $\text{HCO}_3^-$  pool in the presence of functional carboxysomes, with stromal CA eliminated, is predicted to generate a stromal  $\text{HCO}_3^-$  concentration approaching 5 mM<sup>16</sup> and to increase in  $\text{CO}_2$  fixation and yield of up to 60%<sup>15</sup>. c Carboxysomes of *Cyanobium* PCC7001, used in this study, consist of many thousands of polypeptides,



# Construction of a minimal carboxysome in tobacco chloroplasts

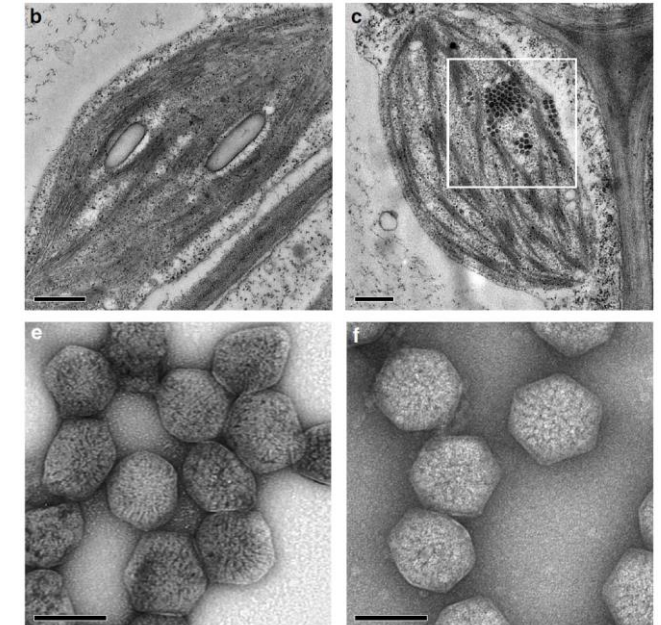
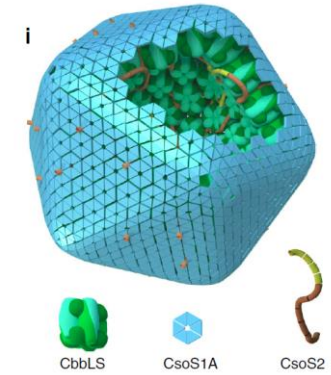
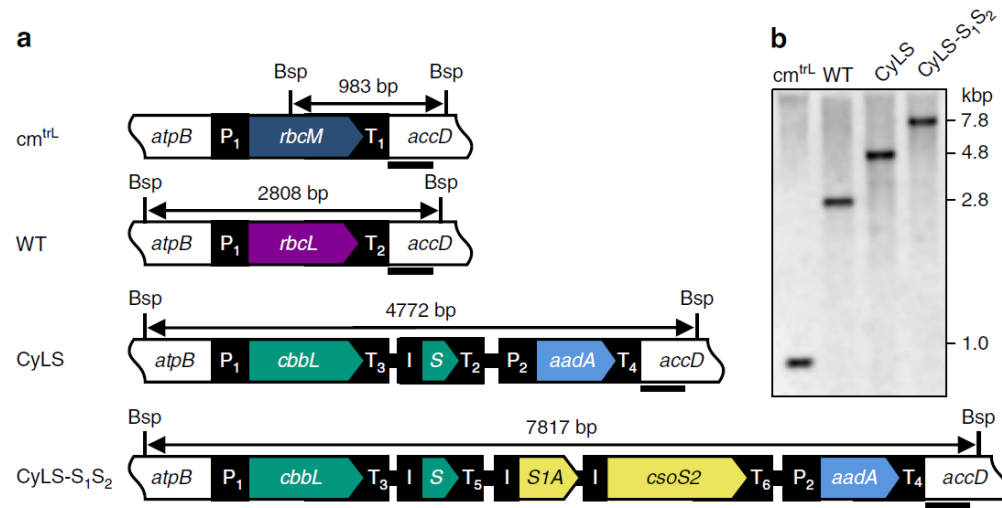
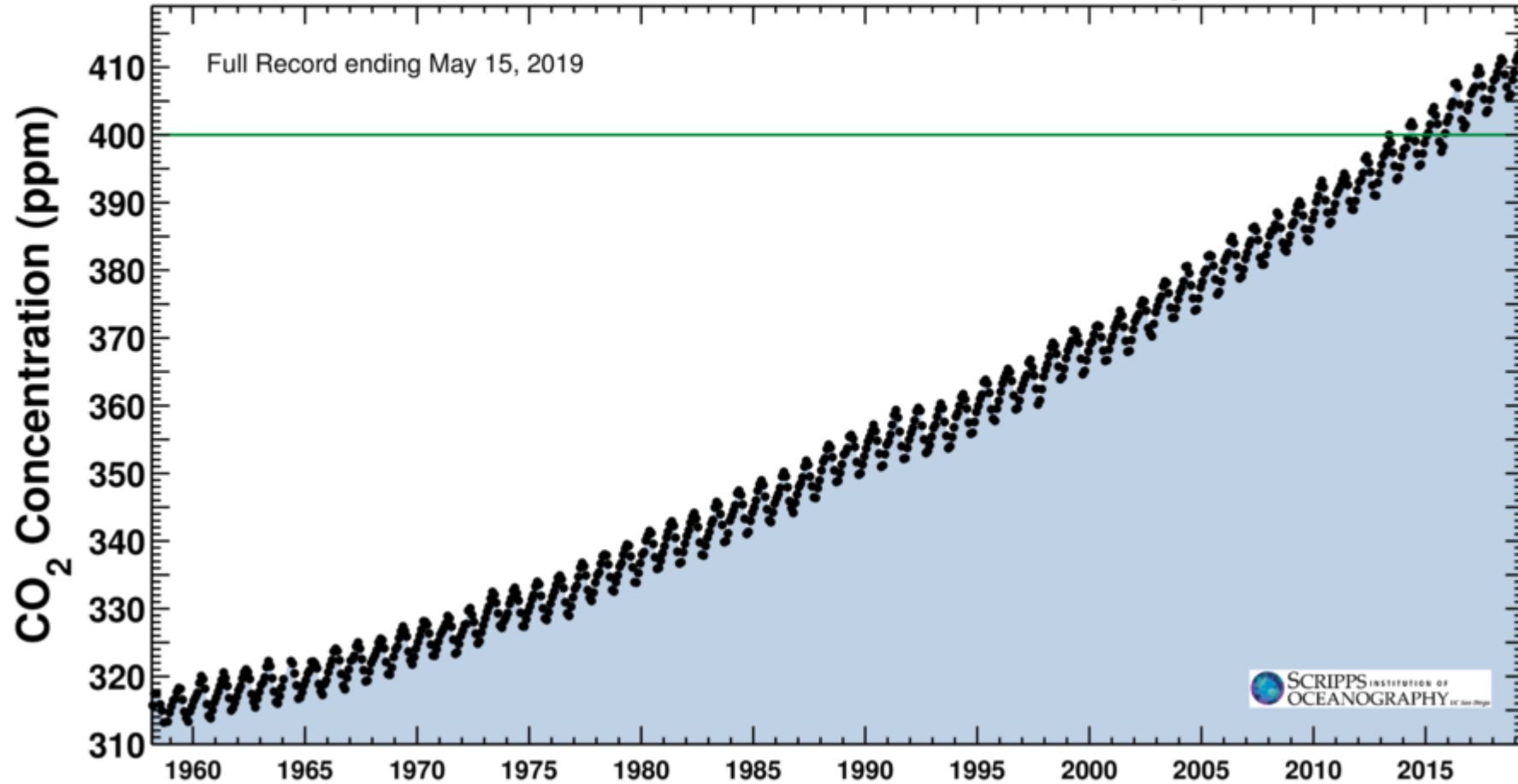


**Fig. 2** Cyanobacterial Form-1A Rubisco and carboxysome gene constructs. **a** Plastome content at the Rubisco large subunit locus in the cm<sup>trL</sup> (*Rhodospirillum rubrum* Rubisco—*rbcM*) master line<sup>37</sup>, wild-type tobacco (WT) and transformant plants (CyLS and CyLS-S<sub>1</sub>-S<sub>2</sub>). The recipient line, cm<sup>trL</sup>, was transformed via homologous recombination with constructs CyLS and CyLS-S<sub>1</sub>-S<sub>2</sub> (GenBank accession numbers MH051814 and MH051815) containing *Cyanobium* PCC7001 Rubisco *cbbL* and *cbbS*, together with carboxysome shell gene *csoS1A* (*S1A*) and *csoS2* sequences, codon optimized for expression in *N. tabacum* chloroplasts. The *Cyanobium cbbL* sequence was also codon matched to the tobacco *rbcL* gene where there was amino acid identity. Transformation vectors also contained the *aadA* selection marker under control of the *NtPpsbA* promoter to allow growth of transformants on spectinomycin. Each transformation construct was flanked by partial plastome *atpB* and *accD* sequence, and transformants were generated using biolistic bombardment. The locations of promoters (P), terminators (T) and intercistronic expression elements (I) are indicated. P<sub>1</sub>, *NtPrbcL*; P<sub>2</sub>, *NtPpsbA*; T<sub>1</sub>, *NtTpsbA* originally from *pcmtrLA*<sup>37</sup>; T<sub>2</sub>, *NtTrbcL*; T<sub>3</sub>, *AtTpetD*; T<sub>4</sub>, *NtTrps16*; T<sub>5</sub>, *AtTpsbA*; T<sub>6</sub>, *CrTrbcL*. A DNA probe was constructed by PCR to anneal to the *accD* flanking region in each plastome (black bar), and the corresponding size of Bsp119I (Bsp) digestion fragments are shown for each genotype (in bp). **b** DNA blots of total leaf DNA digested with restriction enzyme Bsp119I and probed with the *accD* probe, indicating successful insertion of transgenes and loss of the cm<sup>trL</sup> genotype. DNA fragment sizes in kbp are shown

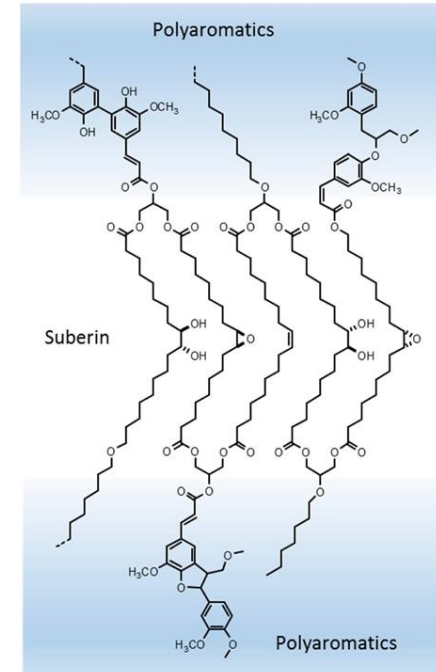
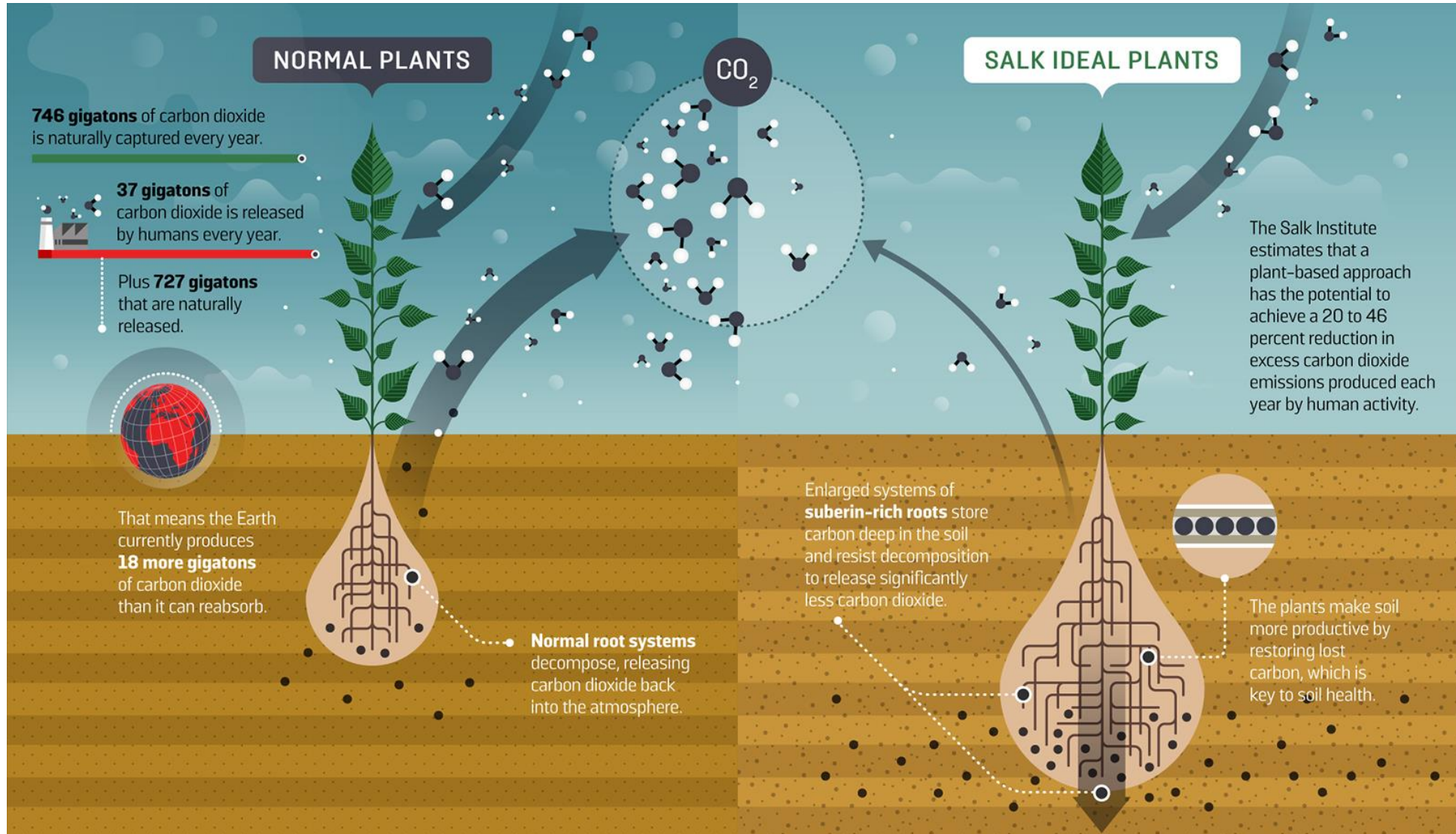
Latest CO<sub>2</sub> reading  
May 15, 2019

415.70 ppm

Carbon dioxide concentration at Mauna Loa Observatory



# SALK superplant to save the planet



Suberin resists decay.

## Recommended reading:

Din M. et al. (2016) Synchronized cycles of bacterial lysis for in vivo delivery. *Nature* 536:81

Kubis A. and Bar-Even A. (2019) Synthetic biology approaches for improving photosynthesis. *J Exp Bot* 70:1425-33